Electrolysis of ammonia for hydrogen production catalyzed by Pt and Pt-Ir deposited on nickel foam

Min Jiang,   Dandan Zhu,   Xuebo Zhao*

The Qingdao Key Lab of Solar Energy Utilization and Energy Storage Technology, Qingdao Institute of Bioenergy and Bioprocess Technology, Chinese Academy of Sciences, Qingdao 266101, Shandong, China

Abstract

Electrolysis of ammonia in alkaline electrolyte solution was applied for the production of hydrogen. Both Pt-loaded Ni foam and Pt-Ir loaded Ni foam electrodes were prepared by electrodeposition and served as anode and cathode in ammonia electrolytic cell, respectively. The electrochemical behaviors of ammonia in KOH solution were individually investigated via cyclic voltammetry on three electrodes, i.e. bare Ni foam electrode, Pt-loaded Ni foam electrode and Pt-Ir loaded Ni foam electrode. The morphology and composition of the prepared Ni foam electrode were analyzed by scanning electron microscopy (SEM) and X-ray diffraction (XRD). Effects of the concentration of electrolyte solution and temperature of electrolytic cell on the electrolysis reaction were examined in order to enhance the efficiency of ammonia electrolysis. The competition of ammonia electrolysis and water electrolysis in the same alkaline solution was firstly proposed to explain the changes of cell voltage with the electrolysis proceeding. At varying current densities, different cell voltages could be obtained from galvanostatic curves. The low cell voltage of 0.58 V, which is less than the practical electrolysis voltage of water (1.6 V), can be obtained at a current density of 2.5 mA/cm^2. Based on some experimental parameters, such as the applied current, the resulting cell voltage and output of hydrogen gas, the power consumption per gram of H$_2$ produced can be estimated.

Key words

ammonia elelctrolysis; nickel electrode; hydrogen produciton; catalyst; power consumption

1. Introduction

A dramatic rise in consumption of fossil energy not only generates large amounts of greenhouse gases and pollutants, but also causes the issues of economics and politics as well as environmental problems, which urge people to search for new fuels. Hydrogen, as a promising energy carrier and the cleanest fuel source, is expected to play a significant role in reducing the dependency on fossil fuels [1]. The most promising application of hydrogen is to be fed into the automotive fuel cell for electricity generation. In general, the hydrogen-fed fuel cell is a kind of devices with higher efficiency than the combustion engines and can generate electric energy to be stored in batteries or to power the electric vehicle [2]. However, as for on-board hydrogen-powered fuel cell system, some technical challenges must be overcome involving the storage and transportation issues of hydrogen gas [3]. One approach is to select less expensive, recyclable, safe materials acting as hydrogen carrier rather than traditional compressed

hydrogen with high pressure constraints or metal hydride with high-temperature dissociation problems [4].

Ammonia has been identified as a suitable hydrogen carrier [5−7]. It has a high hydrogen capacity of 17.6 wt% and boasts a specific energy density 50 percent higher than liquid hydrogen. Moreover, ammonia offers significant advantages in convenience as a vehicular fuel due to its higher density and easier storage and distribution [8,9]. In contrast to other similar hydrogen carriers, such as methanol [10,11], ammonia does not release CO$_x$ during its decomposition which will cause greenhouse effect. In present, there are two feasible ways for ammonia decomposition to produce hydrogen and nitrogen. One is ammonia cracking and the other is ammonia electrolysis. The running of ammonia cracking needs an operation temperature higher than 500 °C and so many issues, such as the longevity and reliability of catalysts, start-up time for the system which are strongly dependent on the operating temperature, and purification requirements to prevent ammonia poisoning of fuel cells as well as efficient reactor designs, must be improved [6,12,13]. Considering on-board practical
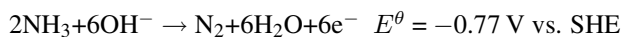
use, the electrochemical process is one of the promising methods to decompose ammonia into hydrogen and nitrogen at a moderate temperature [14,15].

Kojima et al. [16,17] had reported that liquid ammonia was electrolyzed to hydrogen using the metal amide as the supporting electrolyte. The electrolysis voltage of liquid ammonia was theoretically calculated to be 0.077 V which is much lower than the electrolysis voltage of water (1.23 V). Hydrogen molecules were produced and amide ions (NH_2^-) were released at the cathode, while nitrogen molecules were generated by the oxidation of amide ions at the anode. In order to avoid the oxidation and hydration of metal amides, the electrolysis reactor must be designed to be a heavily closed electrolytic cell under the strict experimental conditions. Owing to the inevitable reverse reaction in liquid ammonia, the current efficiency was only 85 percent obtained at a high cell voltage of 2 V [16]. Taking account of the future practical use, attempts must be made on decreasing the cell voltage as low as possible at a high current. Botte group [18] has been working on the electrolysis of alkaline ammonia solution to provide hydrogen for the proton exchange membrane fuel cell (PEMFC). The proposed cell voltage in theory for ammonia electrolysis was only 0.058 V at 25 °C. Ammonia was oxidized in the presence of OH^- at the anode while water was reduced in the alkaline medium at the cathode. Reactions at each electrode and overall reaction are given below.
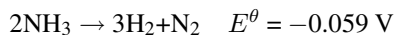
Anode reaction:

$$2NH_3 + 6OH^- \rightarrow N_2 + 6H_2O + 6e^- \quad E^\theta = -0.77 \text{ V vs. SHE}$$

Cathode reaction:

$$2H_2O + 2e^- \rightarrow H_2 + 2OH^- \quad E^\theta = -0.829 \text{ V vs. SHE}$$

Overall reaction:

$$2NH_3 \rightarrow 3H_2 + N_2 \quad E^\theta = -0.059 \text{ V}$$

Botte et al. [19,20] also developed novel catalysts made by electrodeposition of noble metals on carbon fiber paper. And the electrocatalysts reached the current density up to 75 mA/cm^2 at a cell voltage of 0.45 V.

It is well known that the electrode materials and catalysts are of importance to the electrochemical reaction. Therefore, it is meaningful to develop a novel and effective electrode for the generation of hydrogen from ammonia electrolysis applications. Many electrode materials, including noble metal and transition metal, have been tested in order to find the best electrocatalyst for ammonia anodic oxidation [21]. Nickel foam possesses high specific surface area and fine tuned three-dimensional structure which make it a very attractive material for various electrochemical, catalytic and structural applications [22−24]. Furthermore, other attributes of nickel foam such as mechanical strength, relatively low toxicity, and the corrosion stability in aqueous alkaline solution, make it a suitable material for alkaline ammonia electrolysis. The objective of this work is to evaluate the performance of noble metal electrocatalyst deposited on nickel foam substrates for alkaline ammonia electrolysis process. And the following tasks

are involved: (1) to study the feasibility of nickel foam as electrode substrate, (2) to explore the electroplating of anode and cathode with different noble metal catalysts, (3) to investigate the competition of ammonia electrolysis and water electrolysis in the same alkaline solution, (4) to improve the energy consumption of the ammonia electrolyzer.

2. Experimental

2.1. Materials

Chloroplatinic acid hexahydrate ($H_2PtCl_6 \cdot 6H_2O$, 99.9%) and Iridium (III) chloride trihydrate ($IrCl_3 \cdot 3H_2O$) were purchased from Aladdin Industrial Corporation. Potassium hydroxide, concentrated hydrochloric acid (37%), aqueous ammonia solution (28%) and acetone (reagent grade) were purchased from Sinopharm Chemical Reagent Co., Ltd. Nickel foam was provided by Tianjin Incole Union Technology Co., Ltd. Water was obtained from a Millipore system with a resistivity larger than 18 MΩ·cm. All the chemicals were used as received. Ti foil (99%, 0.127 mm in thickness) was purchased from Alfa-Aesar Co., Inc.

2.2. Fabrication of electrodes

Several approaches were employed to treat Ni foams in order to prepare the metallic surfaces. The as-received Ni foams were firstly immersed into acetone for 10 min in order to remove organics, and then sonicated in deionized water for 5 min. The next step involved 15 min immersion period of Ni foam in 6 mol/L HCl solution to remove the surface oxide film. At last, Ni foams were rinsed with amounts of deionized water and dried in the air [25]. Ti framework for supporting Ni foam substrate was tailored from Ti foil with a 12 mm×25 mm hollow center, and 3 mm in edge width. The cleaned Ni foams were cut into rectangular (11 mm×25 mm) and inserted into the as-prepared Ti framework as deposition electrode. It is well known that the overpotential of hydrogen evolution on Pt cathode in basic medium is low so that Pt-loaded Ni foam substrate was served as cathode in this work [26]. And some reports have proved that Pt-Ir binary system has the ability of improving the electrocatalytic activity for ammonia oxidation [27]. This is the reason of preparing a Pt-Ir bimetallic deposited Ni foam for the anode. The electrodepositions of Pt and Pt-Ir on nickel foam substrate were performed in two different plating solutions at room temperature. The anode plating bath was prepared by dissolving the required quantities of $H_2PtCl_6 \cdot 6H_2O$ and $IrCl_3 \cdot 3H_2O$ salts (keeping a weight ratio of 7 : 1, Pt to Ir) in 0.5 mol/L HCl solution. The cathode plating solution was composed of 5 mmol/L H_2PtCl_6 and 0.5 mol/L HCl solution. The plating was performed by Amperometric *i-t* curve at a potential of −0.3 V for 3600 s in a conventional one-compartment cell with saturated calomel electrode (SCE) as a reference electrode and Pt wire as an auxiliary electrode. Such as-prepared electrodes were served as anode and cathode for ammonia electrolysis,

respectively, in the electrolytic cell filled with 2 mol/L ammonia and 1 mol/L/5 mol/L KOH aqueous solution. A Pt plate electrode (10 mm×20 mm) was used for comparative trial.

2.3. Characterization

Electrochemical experiments were carried out on a Model 660D Voltammetric Analyzer (CHI Instruments, USA). Scanning Electron Microscopy (SEM) images were obtained with a Hitachi S-4800 (Japan) scanning electron microscope at an acceleration voltage of 15 kV. X-ray diffraction (XRD) patterns were collected by a Bruker D8 Advance X-ray diffractometer using Cu K_α radiation ($\lambda = 0.154$ nm). The electrolysis of ammonia was performed in a home-made H type electrolytic cell with a glass sand circle as connector as shown in Figure 1. The solution volume in each cell was 50 mL. Each cell was closed by a Teflon cap with a hole for electrode insertion and a gas outlet. The gas collection and measurement equipment involves a gas burette and a glass bottle controlling water level. In order to keep the pressure in gas burette at atmosphere pressure all along, the height of water level bottle should be adjusted at any time during the gas production. The amount of the produced hydrogen or nitrogen was equal to the decrease value of water level in gas burette.
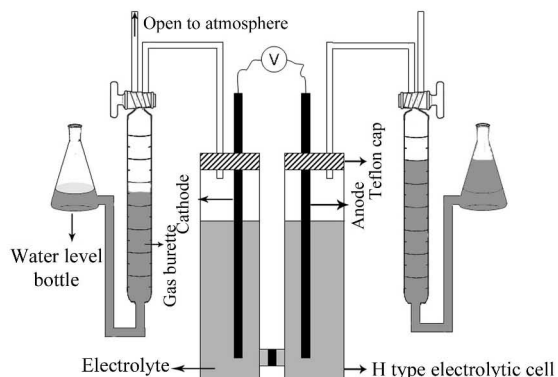

Figure 1. Schematic of H type ammonia electrolytic cell with gas measurement part

3. Results and discussion

3.1. Electrochemical behavior of anode and cathode

Cyclic voltammetry (CV) was utilized to investigate the electrochemical activity of ammonia in alkaline solution. Figure 2 shows four cyclic voltammograms obtained on a cleaned Pt plate, a cleaned Ni foam electrode, a Pt-loaded Ni foam electrode and a Pt-Ir loaded Ni foam electrode, respectively.

As shown in Curve a, the cathodic peak around −1.0 V corresponds to the adsorption of hydrogen on the clean Pt plate electrode [28]. A sharp increase in current is caused by amounts of hydrogen evolution at a potential of −1.2 V. In the

following reverse process, adsorbed hydrogen was reoxidized with appearance of anodic peak near −1.0 V and the anodic peak around −0.4 V can be assigned to the oxidization of ammonia to nitrogen [29]. At more positive potential over 1.0 V, OH^- ions could lose four electrons and release one oxygen molecule with the rapid increase of anodic current. As shown in Curve b, no evolution and desorption peak of hydrogen was observed around a potential of −1.2 V, which proves the potential of hydrogen evolution is high on pure nickel substrate in alkaline ammonia solution. In the same case, ammonia cannot be oxidized on the surface of bare nickel electrode without any peak of ammonia oxidation shown in CV [30]. One well-defined set of peak ($E_{ap} = 0.34$ V and $E_{cp} = 0.16$ V) in Curve b corresponds to the reversible two-electron redox process, where Ni^0 is oxidized to Ni^{2+} in the form α-$Ni(OH)_2$ and reversely α-$Ni(OH)_2$ is reduced to Ni^0 [31−33]. It is visible that the original Ni foam with silver color changed to uniform black (the color of α-$Ni(OH)_2$) with the increasing potential and the color recovered from black to silver in the reverse process. When Pt was electrodeposited on the surface of nickel foam substrate, the peaks became very obvious, corresponding to the hydrogen generation and ammonia oxidization as shown in Curve c. It reveals that electrodeposited Pt plays an important role in electrocatalyzing the ammonia electrolysis and correspondingly it functionalizes nickel foam electrode. The same electrocatalysis effect was also observed in Curve d using a Pt-Ir bimetallic deposited Ni foam working electrode. In contrast to the potential of ammonia oxidation in Curve c, that in Curve d shifted to the positive one. It gives us the information that Pt-Ir bimetallic deposited Ni foam electrode is more suitable for serving as anode to accelerate ammonia oxidation.
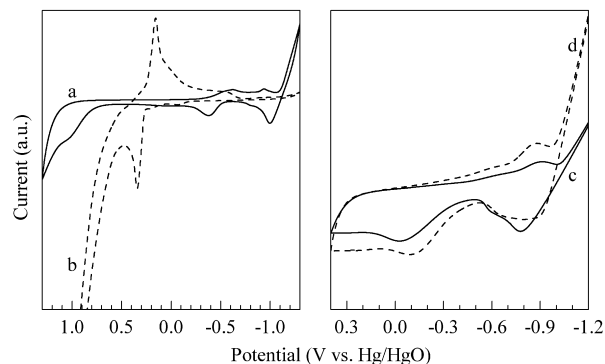

Figure 2. Cyclic Voltammetry of a cleaned Pt plate (Curve a), a cleaned Ni foam (Curve b), a Pt-loaded Ni foam electrode (Curve c) and a Pt-Ir loaded Ni foam electrode (Curve d) in 2 mol/L NH_3/1 mol/L KOH electrolyte solution at 25 °C. Scan rate: 0.1 V/s

3.2. Surface morphology and component analysis of electrode

The morphology of electrode surface was characterized using microscopy technique. Figure 3(a) shows an SEM micrograph of cleaned Ni foam which revealed the existence

of interconnected struts that generated small and large open pores with ca. 100 ± 20 μm and 500 ± 100 μm in size, respectively [34]. The enlargement of strut section in clean Ni structure exhibited a flat surface without any protuberances in Figure 3(b). When Pt or Pt-Ir was electrodeposited onto Ni substrate, different structures formed on the strut surface, as shown in both Figure 3(c) and 3(e). After Pt was electrode-

posited onto Ni substrate, it can be obviously observed from Figure 2(d) (the enlargement of Figure 3c) that a lot of slices piled up on the strut surface of Ni foam electrode with a uniform coverage. The electrodeposits of Pt and Ir formed some phase separation domains on strut surface, as shown in Figure 3(e). And some small particles existed in the domains, as shown in Figure 3(f).
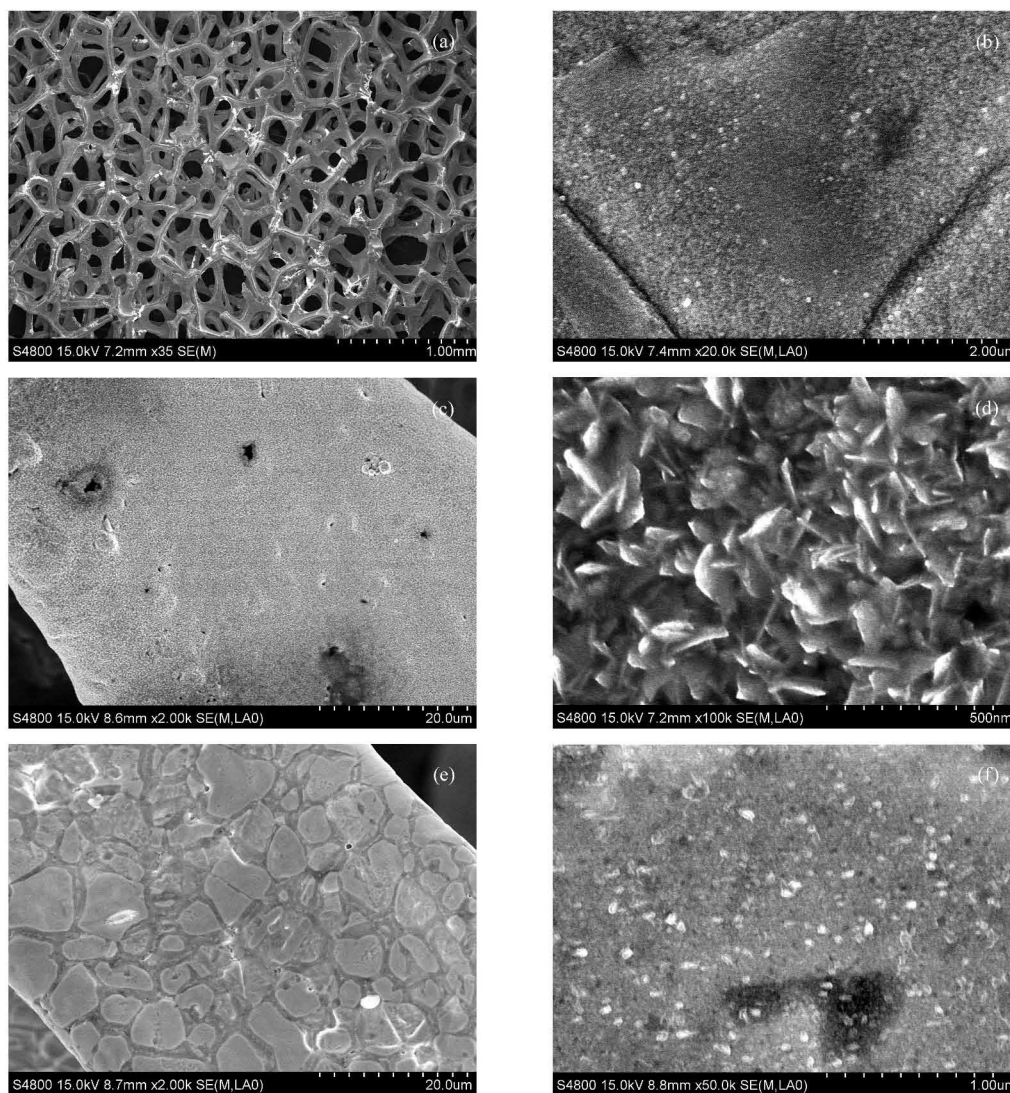

Figure 3. SEM micrographs of (a) the apparent surface of cleaned Ni foam, (b) the strut surface inside cleaned Ni foam, (c) the strut surface inside Pt-deposited Ni foam, (d) the enlargement of (c), (e) the strut surface inside Pt-Ir-deposited Ni foam and (f) the enlargement of (e)

Figure 4 illustrates the XRD patterns of Pt and Pt-Ir deposited on nickel foam. The main characteristic peaks of Ni substrate marked with three black square symbols can be obviously observed. Four small peaks assigned to Pt were labeled with *hkl* indexes in Curve a. The first peak Pt(111) was visible, while the other three peaks can be observed from the magnification of blank column in the patterns. The addition of Ir led to an increase in the relative intensities of the reflections as shown in Curve b, which was in good agreement with the results obtained from Pt-Ir film in Ref. [35].

3.3. Decomposition voltage of ammonia

A step voltage test was used to find the decomposition voltage of ammonia in electrolysis reaction according to the change of resulting current. The resulting current-time (i-t) curves were displayed in Figure 5(a) when a 0.1 V step was applied for a potential increase from 0.1 to 0.7 V. When the applied potentials were below 0.4 V, the currents were much less than 10 mA and the settling time to reach a steady value was short. A sharp decrease of current within initial $5-10$ s
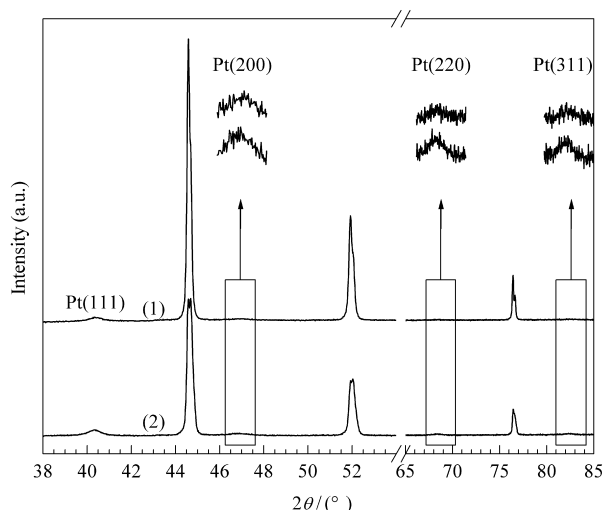
Figure 4. XRD patterns of Pt-deposited Ni foam (1) and Pt-Ir deposited Ni foam (2)

mainly results from the growth of the diffusion layer near the electrode. When the potential was enhanced to 0.5 V, a small increment in current value was visible.

It is interesting to notice that further increasing the applied potential to 0.6 V caused an obvious enhancement of current value. Likewise, the current quickly reached a stable value and kept it all along. It clearly demonstrates that the actual decomposition voltage of ammonia was in the range of 0.5 V and 0.6 V. Moreover, the increase of applied potential resulted in the increase of electrolysis current, however, it would take a longer period for the resulting current to decay to a steady value (see the curve obtained at 0.7 V). The inset in Figure 5(a) shows the plot of the steady current value as a function of the applied potential. When the applied voltage was set at a value larger than 0.8 V, the current resulted kept a steady value. It is possible that the electrochemical electron transfer process occurs in Ni foam substrate under a relative high applied potential in addition to the electrolysis reaction of ammonia for hydrogen production.
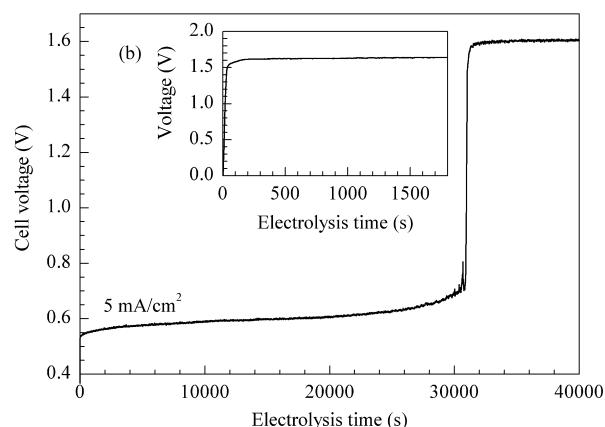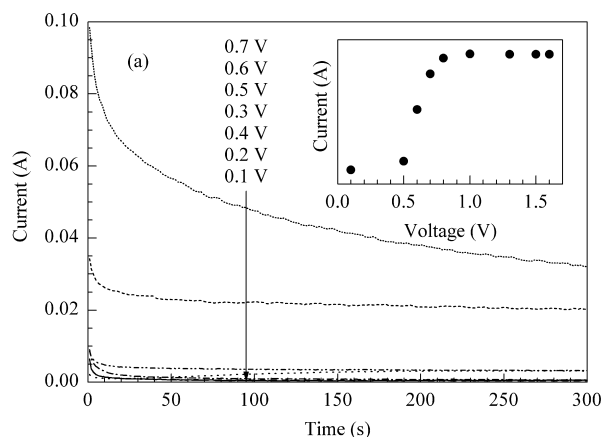

Figure 5. (a) Amperometric *i-t* curves during the electrolysis of ammonia processes in 2 mol/L NH_3/1 mol/L KOH solution at 25 °C obtained at different applied potentials. The inset shows plot of the current as a function of applied potential in the electrolytic cell; (b) Galvanostatic curve obtained at a current density of 5 mA/cm^2 at 25 °C in the electrolytic cell filled with 2 mol/L NH_3/5 mol/L KOH solution. The inset presents the galvanostatic response in an electrolytic cell filled with 5 mol/L KOH aqueous solution using the same electrodes
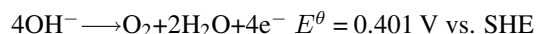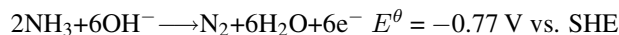
Galvanostatic curve is another method for studying the decomposition voltage of ammonia in electrolysis reaction. Figure 5(b) displays the galvanostatic curve obtained at a current density of 5 mA/cm^2. With the proceeding of electrolysis reaction, the cell voltage of ca. 0.55 V at the beginning gradually increased until the voltage of 0.8 V was achieved for a 9-hour period. Then a drastic lift of cell voltage occurred and another plateau on galvanostatic curve formed. Such a changing process was controlled by several factors. First, the slow increase trend in potential was related to the gradual consumption of ammonia and mass-transfer limitation near the electrode. Use of high concentrated electrolyte solution would speed the electron transfer to weaken the change of cell voltage caused by ammonia consumption. The corresponding evidence was provided in the following Section 3.4. Second, similar phenomena of the sharp increase in potential were observed and explained in Ref. [36]. The author pointed out that it was due to the complete consumption of ammonia species

in solution. However, according to the galvanostatic curve measurements in our electrolysis system, the cell voltage each time still kept steady for a long period of time before a sharp increase appeared again while the electrolyte solution was not renewed. It illustrates that the ammonia species in solution are not consumed completely and other reasons should be considered to explain our results. We think of that the electrolysis of water in the same electrolytic cell may be the other important factor. In fact, the difference between the electrolysis reaction of ammonia and water in alkaline solution is just anode reaction, while their cathode reaction is the same. From the following two anode reactions, it is obvious that the competition between NH_3 and OH^- plays a critical role in deciding which reaction does happen in alkaline solution. At the beginning, NH_3 molecules adsorbed on the surface of electrode and then were oxidized to give N_2. With the electrolysis proceeding, a greater number of OH^- occupied the active sites on the electrode, the oxidation of ammonia could be blocked so that

the oxygen will be produced instead of N_2 at anode.

$$2NH_3 + 6OH^- \longrightarrow N_2 + 6H_2O + 6e^- \quad E^\theta = -0.77 \text{ V vs. SHE}$$

$$4OH^- \longrightarrow O_2 + 2H_2O + 4e^- \quad E^\theta = 0.401 \text{ V vs. SHE}$$

At a constant current density, the cell voltage will gradually increase to keep the electrolysis reaction continuing because of the consumption of ammonia near the electrode surface. Simultaneously, OH^- competes with NH_3 for adsorption on the electrode surface which will finally block the electro-oxidation of amminia, and trigger the electrolysis of water at 1.6 V for the production of hydrogen and oxygen. In addition, a porous Ni electrode used in this work may be responsible for the increase in overpotential, but the definite reason is not clear.

To certify the electrolysis of water proceeding with the appearance of the second plateau on galvanostatic curve at the voltage of 1.6 V, an alkaline aqueous solution without ammonia was electrolyzed in the same electrolytic cell using the same electrodes. The resulting cell voltage is just 1.6 V which can be obviously concluded from the inset of Figure 5(b). In order to avoid the electrolysis of water in ammonia solution, the rest tests run until the cell voltage reaches a level of 1.2 V.

3.4. Optimization of electrolysis process

In general, the deposition amount of noble metal on the substrate has an important influence on the electrochemical process. And the deposition amount is always dependent on the deposition time. Two deposition times were chosen for both Pt and Pt-Ir electrodeposition onto Ni foam substrate. Galvanostatic curves in Figure 6(a) were obtained using noble metal-loaded Ni foam electrode prepared by 600 s and 3600 s electrodeposition, respectively. In comparison, it was found that the curve obtained from the electrode with a deposition time of 3600 s showed a better catalytic role than that with a deposition time of 600 s in electrolytic cell. Obviously, the more noble metal deposited on the surface of Ni foam, the longer durability of the whole Ni electrode was. However, the increase of noble metal loading will certainly raise the fabrication cost of the electrode in practical electrolysis process. Besides the electrodeposition time affects the durability of electrolytic cell, it also has a clear influence on the rate of hydrogen production. We will discuss this point later.

The operation temperature of electrolytic cell will affect the cell voltage. Figure 6(b) displays the voltage of electrolytic cell at different temperatures. At 25 °C, the cell voltage could not sustain at a steady potential even at a current density as small as 2.5 mA/cm^2. However, it can be seen that a trial at the same current density (2.5 mA/cm^2) at 60 °C could maintain a relative steady voltage at least 9 h. This result demonstrates that higher temperature of electrolyte solution benefits the transfer of electron in the process of the electrolysis of ammonia so as to optimize performance of the noble metal deposited Ni foam electrodes.
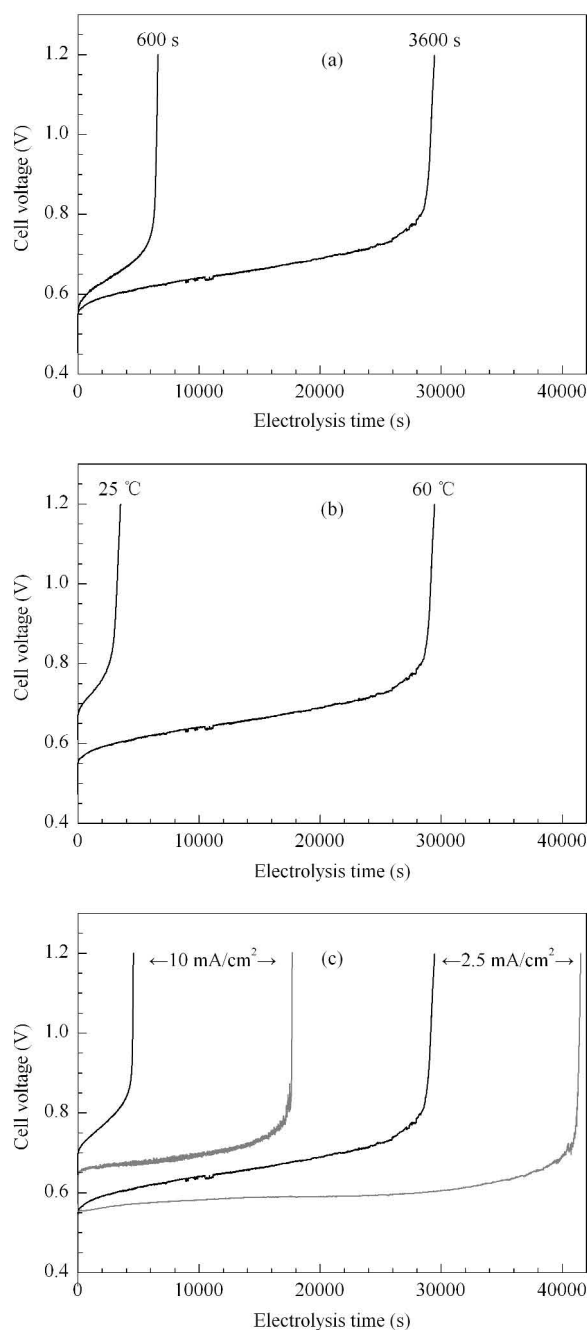

Figure 6. (a) Galvanostatic curves obtained at a current density of 2.5 mA/cm^2 of the electrolytic cell under 60 °C filled with 2 mol/L NH$_3$/1 mol/L KOH solution. The electrodeposition time of noble metal on Ni foam substrates was 600 s and 3600 s, respectively. (b) Galvanostatic curves obtained at a current density of 2.5 mA/cm^2 of the electrolytic cell filled with 2 mol/L NH$_3$/1 mol/L KOH solution at different temperatures. (c) Galvanostatic curves obtained at different current densities of 10 mA/cm^2 and 2.5 mA/cm^2 in the electrolytic cell filled with 2 mol/L NH$_3$/1 mol/L KOH solution (black line) and 2 mol/L NH$_3$/5 mol/L KOH solution (gray line)

As aforementioned Section 3.3, it is a better approach to sustain a constant voltage for a long time by increasing the concentration of electrolyte solution. Clearly, the galvanostatic curves obtained in 5 mol/L KOH electrolyte solution (two gray lines in Figure 6c), show much more steady and longer period than those obtained in 1 mol/L KOH electrolyte solution (two black lines in Figure 6c). Moreover, the cell

voltage associated with the application of 2.5 mA/cm^2 current density could sustain at a constant potential for more than 11 h. It can be attributed to that the electrolyte with high concentration can benefit the transfer of electron to/from the electrode surface so as to alleviate the influence of ammonia concentration near electrode which always causes the increase of cell voltage at a fixed current. Actually, the role of increasing the temperature and concentration of electrolyte solution is nearly the same for enhancing the electrolysis reaction in alkaline ammonia electrolytic cell.

3.5. Hydrogen production and energy consumption

The hydrogen production from the electrolysis of ammonia is of significance to judge the quality and efficiency of the electrolytic cell. Therefore, the production of gases on anode and cathode was monitored, respectively. As shown in Figure 7(a), the generation volume ratio of H$_2$ to N$_2$ was near 3 : 1 during one hour monitoring. The result is consistent with the theoretical molar ratio of H$_2$ to N$_2$ from the ammonia electrolysis reaction in alkaline solution [19]. Additionally, the
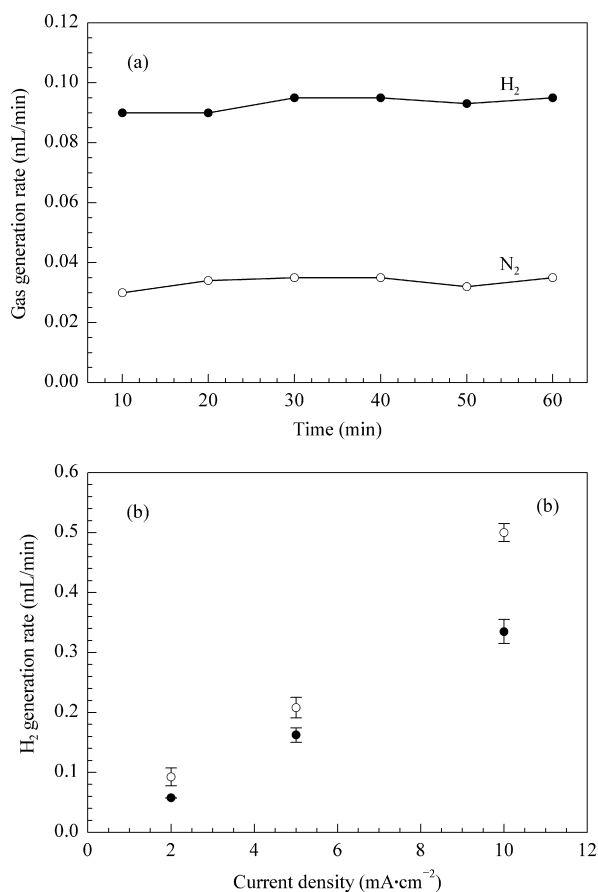

Figure 7. (a) Measurements of the generation rate of hydrogen and nitrogen as a function of electrolysis time operated in the alkaline ammonia electrolytic cell at a current density of 2.5 mA/cm^2. (b) Hydrogen production rate from ammonia electrolysis as a function of current density using Ni foam cathodes loaded with different amounts of noble metals. The electrodeposition time of noble metals on Ni foam substrate was 600 s (solid symbol) and 3600 s (hollow symbol), respectively

generation rate of hydrogen is affected by the catalytic role of loaded noble metal and applied current density. It is clearly seen from Figure 7(b) that the rate of hydrogen production depends on the loading amount of noble metal at any current density, as aforementioned Section 3.4. In other words, the longer the deposition time of noble metal, the higher the output of hydrogen was. Moreover, high current density helps to enhance the rate of ammonia decomposition and also speed up the rate of hydrogen production. However, the stability and sustainability of electrolytic cell must be considered at high current density.

Based on the above results, the optimal experimental conditions (5 mol/L KOH solution and operation temperature of 60 °C) were utilized to realize the galvanostatic response at different current densities. As shown in Figure 8, the cell voltage could not maintain a long steady state and it took only 2 h to reach a sharp rising level at a high current density of 20 mA/cm^2. As for 10 mA/cm^2 current density, the situation has been improved and there was a plateau of the cell voltage sustains for at least 5 h. When the current density was controlled at 5 mA/cm^2, the cell voltage can be stabilized for about 10 h. Moreover, the cell voltage obtained at 2.5 mA/cm^2 seemed more sustainable so that the electrolytic cell performed well under this condition. Hence, the cell voltage achieved at a current density of 2.5 mA/cm^2 was adopted to calculate the energy consumption of ammonia electrolysis reaction.
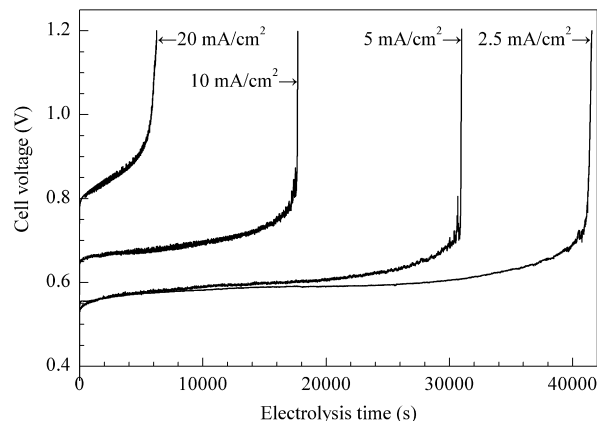

Figure 8. Galvanostatic curves obtained at varying current densities in the electrolytic cell filled with 2 mol/L NH$_3$/5 mol/L KOH solution at 60 °C

Considering the future integration of ammonia electrolytic cell and PEMFC to achieve high net energy for motors, the power consumption of ammonia electrolysis is not neglectable. According to the power formula of $P = UI$, as the voltage associated with a constant applied current decreases, the energy consumption to generate hydrogen will be reduced proportionally [36]. At a current density of 2.5 mA/cm^2, the corresponding cell potential was 0.58 V. Regarding that the electro-oxidation of ammonia has 100% efficiency, it can be theoretically calculated that the electric power for 1 g H$_2$ production from ammonia electrolysis takes ca. 15.5 Wh. But the actual power consumption

was 17.6 Wh/g H_2 based on the above mentioned real volume of hydrogen. The difference between theoretical power consumption and real consumption is caused by two main reasons. One is that the current efficiency of ammonia electro-oxidation is always below 100%. The other is that relative less amount of hydrogen generation at 2.5 mA/cm^2 easily make some experimental errors by this home-made setup. The same calculation methods can be applied to other results obtained at a current density of 5 mA/cm^2. The theoretical power consumption of 15.8 Wh/g H_2 is larger than the actual power consumption of 14.8 Wh/g H_2 at 5 mA/cm^2. Such a result can be utilized to estimate that mixing of water or ammonia vapor into the generated hydrogen results in the increase of hydrogen volume measured. Further decrease of the experimental electrolysis voltage at a high current density will be beneficial to the practical use on fuel cell. Its realization depends on the development of effective electrode materials in future.

4. Conclusions

The electrolysis of ammonia in alkaline electrolyte solution for hydrogen production has been performed successfully using a Pt-Ir bimetallic electrodeposited Ni foam substrate as anode and a Pt-deposited Ni foam electrode as cathode. High concentration and temperature of electrolyte solution benefit the stability and sustainability of electrolysis reaction in alkaline ammonia electrolyzer. Likewise, increasing the electrodeposition time helps the electrodes to enhance the rate of ammonia decomposition and also speed up the rate of hydrogen production. Low cell voltage of 0.58 V can be obtained at a current density of 2.5 mA/cm^2 which is greatly less than the practical electrolysis voltage of water (1.6 V), but it exceeds the theoretical electrolysis voltage of 0.058 V a great deal. The competition between NH_3 and OH^- results in the transition of electrolysis reaction from ammonia electrolysis to water electrolysis in the alkaline electrolytic cell with the increase of cell voltage. As for the practical use, the applied current density must be further increased on the premise of sustaining the low cell voltage and the durability of the whole electrolytic cell. Taking these points into account, intensive study now is underway in our group.

References

[1] Lubitz W, Tumas W. *Chem Rev*, 2007, 107(10): 3900
[2] Schlapbach L, Zuttel A. *Nature*, 2001, 414(6861): 353
[3] Jensen J O, Vestbø A P, Li Q, Bjerrum N J. *J Alloys Compd*, 2007, 446-447: 723
[4] Orimo S, Nakamori Y, Eliseo J R, Zuttel A, Jensen C M. *Chem Rev*, 2007, 107(10): 4111

[5] Christensen C H, Johannessen T, Sørensen R Z, Nørskov J K. *Catal Today*, 2006, 111(1-2): 140
[6] Faleschini G, Hacker V, Muhr M, Kordesch K, Aronsson R R. 2000 Fuel Cell Seminar, Portland, 2000. 336
[7] Hejze T, Besenhard J O, Kordesch K, Cifrain M, Aronsson R R. *J Power Sources*, 2008, 176(2): 490
[8] Saika T, Nakamura M, Nohara T, Ishimatsu S. *Jsme Int J Ser B-Fluid Thermal Eng*, 2006, 49(1): 78
[9] Kordesch K, Hacker V, Gsellmann J, Cifrain M, Faleschini G, Enzinger P, Fankhauser R, Ortner M, Muhr M, Aronson R R. *J Power Sources*, 2000, 86(1-2): 162
[10] Mehri F, Taghizadeh M. *J Nat Gas Chem*, 2012, 21(5): 526
[11] Xu D Y, Zhao L, Dai P, Ji S F. *J Nat Gas Chem*, 2012, 21(5): 488
[12] Hacker V, Kordesh K. In: Vielstich W ed. Handbook of Fuel Cells. Chichester: Wiley & Sons, 2003. 121
[13] Thomas G, Parks G. Potential Roles of Ammonia in a Hydrogen Economy, U.S. Department of Energy, 2006
[14] Vitse F, Cooper M, Botte G G. *J Power Sources*, 2005, 142(1-2): 18
[15] Muthuvel M, Botte G G. In: White R E ed. Modern Aspects of Electrochemistry, 45. New York: Springer, 2009. 207
[16] Hanada N, Hino S, Ichikawa T, Suzuki H, Takai K, Kojima Y. *Chem Commun*, 2010, 46(41): 7775
[17] Dong B X, Ichikawa T, Hanada N, Hino S, Kojima Y. *J Alloys Compd*, 2011, 509(S2): S891
[18] Boggs B K, Botte G G. *J Power Sources*, 2009, 192(2): 573
[19] Bonnin E P, Biddinger E J, Botte G G. *J Power Sources*, 2008, 182(1): 284
[20] Botte G G. US patent 0252422A1. 2010
[21] de Vooys A C A, Koper M T M, van Santen R A, van Veen J A R. *J Electroanal Chem*, 2001, 506(2): 127
[22] Grdeń M, Alsabet M, Jerkiewicz G. *ACS Appl Mater Interfaces*, 2012, 4(6): 3012
[23] Rausch S, Wendt H. *J Electrochem Soc*, 1996, 143(9): 2852
[24] Jeremiasse A W, Hamelers H V M, Saakes M, Buisman C J N. *Int J Hydrog Energy*, 2010, 35(23): 12716
[25] Yuan C Z, Li J Y, Hou L R, Zhang X G, Shen L F, Lou X W. *Adv Funct Mater*, 2012, 22(21): 4592
[26] Jaksic M M, Johansen B, Tunold R. *Int J Hydrog Energy*, 1993, 18(10): 817
[27] Endo K, Katayama Y, Miura T. *Electrochim Acta*, 2004, 49(9-10): 1635
[28] Gerischer H, Mauerer A. *J Electroanal Chem*, 1970, 25(3): 421
[29] Katan T, Galiotto R J. *J Electrochem Soc*, 1963, 110(9): 1022
[30] Kapalka A, Cally A, Neodo S, Comninellis C, Wachter M, Udert K M. *Electrochem Commun*, 2010, 12(1): 18
[31] Hahn F, Floner D, Beden B, Lamy C. *Electrochim Acta*, 1987, 32(11): 1631
[32] Grden M, Klimek K. *J Electroanal Chem*, 2005, 581(1): 122
[33] Wang Y, Cao D X, Wang G L, Wang S S, Wen J Y, Yin J L. *Electrochim Acta*, 2011, 56(24): 8285
[34] Paserin V, Marcuson S, Shu J, Wilkinson D S. *Adv Eng Mater*, 2004, 6(6): 454
[35] Topalov G, Ganske G, Lefterova E, Schnakenberg U, Slavcheva E. *Int J Hydrog Energy*, 2011, 36(23): 15437
[36] Cooper M, Botte G G. *J Electrochem Soc*, 2006, 153(10): A1894